

**Persistence and transmission dynamics of emerging tick-borne pathogens:
Extending a 2-pathogen, 1-host, 1-vector SIR metapopulation model**

Hubert Pan¹, Dorian Feistel¹, and Matthew H. Seabolt¹

¹School of Biological Sciences, Georgia Institute of Technology, Atlanta GA, 30332

ABSTRACT

Novel extensions to a published SIR compartment model describing the dynamics of vector-borne disease in a 2-pathogen/1-vector/1-host system are described and implemented. The goals of these model extensions are to analyze the resulting changes to the transmission dynamics of two established pathogens induced by the introduction of novel diversity in the form of either a newly emerged (i.e. competing) pathogen or the expansion of the pathogens' ecological niche to new vectors and new hosts. While our proposed model extensions are theoretical by design, we obtained plausible initial values gleaned from real-world case studies of applicable vector-borne model systems in an effort to demonstrate realistic parameter ranges that may underly similar biological systems as they occur in nature. Extended epidemic models such as those included in this study have potential to become valuable tools in the public health science toolbox by helping scientists and decision-makers evaluate threats posed by -for example- the emergence of new vector-borne pathogens or by the expansion of the host or geographic range of established pathogens due to climate change.

Keywords: SIR models, transmission dynamics, vector-borne diseases, metapopulation models, mathematical biology

1. INTRODUCTION

The diversity and zoonotic potential of tickborne diseases has been reported with increasing frequency over the past decade, increasing the threat to human and veterinary health (Rondino et al. 2020). Ticks belong to the arachnid order and are classified into two broad types: hard-bodied ticks (family Ixodidae) and soft-bodied ticks (family Argasidae) (Durden and Beati 2013). The ixodid ticks are the most common ectoparasites of humans and mammals in the United States with an average of approximately 50,000 cases of tickborne diseases reported each year by multiple species of this group, estimated to be 77-95% of the reported cases of vector-borne disease (Rondino et al. 2020; [cdc.gov/ticks/data-summary](https://www.cdc.gov/ticks/data-summary), accessed 2022-10-04). The tick life cycle includes three obligate parasitic stages: larva, nymph, and adult. Each stage is characterized by the need for a blood meal from a suitable host, during which the feeding tick attaches to the host, consumes a meal, and then detaches to molt to the next stage (Figure 1, right). During this feeding process, some pathogens, such as *Rickettsia spp.* (spotted fevers), *Borrelia burgdorferi* (Lyme disease), and *Ehrlichia chaffeensis* (heartwater), which are present in the host, can be transmitted to the feeding tick via the consumed blood meal (Madison-Antenucci et al. 2020). Following host-to-tick transmission, the pathogen(s) colonize the mid- or hindgut of the tick and can be further transmitted by the tick vector to new hosts on which the infected tick feeds ([cdc.gov/ticks/life_cycle_and_hosts](https://www.cdc.gov/ticks/life_cycle_and_hosts), accessed 2022-10-04). Once colonized (=“infected”), molting larvae or nymphal ticks retain the commensal pathogen as they advance to their next life stage (known as trans-stadial transmission). Similarly, adult

female ticks can vertically transmit infection to her offspring when eggs are laid (called trans-ovarial transmission), thus the newly hatched larvae are infectious prior to consuming any blood meal and capable of tick-to-host transmission when they attach to their first host (Rondino et al. 2020).

Modelling vector-borne disease with compartment models such as SIR represents a powerful way to examine population dynamics of tick vectors and the zoonotic pathogens they transmit. The standard SIR model can be extended to capture unique dynamics of vector-borne pathogen transmission, including published models which reflect the multiple modes of transmission and additional states/compartments required to accurately describe a biological system that includes the vector(s), host(s), and the infectious agent(s) at play (White et al. 2019). Further extensions to these existing compartment models can better portray the populations dynamics and expected pathogen persistence, defined as the pathogen's ability to survive disturbances, as they occur in nature by attempting to capture additional parameters of natural systems and using fewer simplifying assumptions. In this proposal, we will analyze a published 2-pathogen/1-vector/1-host compartment model (hereafter referred to as the "2-1-1" model) which models the dynamics of two species of rickettsial pathogen, the tick vector *Amblyomma*, and the white-tailed deer host. We aim to extend the deterministic differential equations (ODEs) underlying this model to include additional pathogens, vectors, and hosts with an eye towards better understanding the epidemic potential, transmission dynamics, and persistence of the competing pathogen species as additional diversity is introduced into the model. While theoretical, our proposed extensions to the 2-1-1 model may be useful to examine potential scenarios of public health concern such as emerging zoonoses as "old" pathogens expand their ecological niche by gaining new vectors or host species, or in which they may be outcompeted by the introduction of new pathogens.

2. MODEL CONCEPTUALIZATION: Extending a 2 pathogen, 1 vector, 1 host model to 2 pathogens, 2 vector, 1 host (2-2-1) model as proof-of-concept

2.1 Population Dynamics

Let N be the population size of white tailed deer hosts, K represents the carrying capacity of the environment, and β is the birth rate of the deer population. Additionally, let V represent the Vector population size (*Amblyomma spp.* ticks), $\hat{\beta}$ represents the density-dependent vector birth/death rate, M is the maximum number of ticks per host, and b is the density-independent death rate.

Thus, Equations 1 and 2 model the initial host and vector population dynamics, respectively.

$$\frac{dN}{dt} = \beta \left(\frac{K - N}{K} \right) N - bN \quad (1)$$

$$\frac{dV}{dt} = \hat{\beta} \left(\frac{MN - V}{MN} \right) V - \hat{b}V \quad (2)$$

2.2 Tick-to-Host Transmission Dynamics

Let A_i be the rate of transmission from tick to host and include the biting rate, probability of transmission, and proportion of hosts to ticks. $\left(\frac{N - Y_1 - Y_2 - Y_{12}}{N} \right)$ is the uninfected population divided by total population - $(X_i + X_{12})$ is the number of vectors infected with pathogen i (including the coinfecting

vectors), shown in Equation 3. Equation 4 extends this simplified transmission dynamic to include general tick-to-host transmission with two pathogen system.

$$A_i \left(\frac{N - Y_1 - Y_2 - Y_{12}}{N} \right) (X_i + X_{12}) \quad (3)$$

$$\frac{dY_1}{dt} = A_1 \left(\frac{N - Y_1 - Y_2 - Y_{12}}{N} \right) (X_1 + X_{12}) + v_{12,1} Y_{12} - A_{12} \left(\frac{Y_1}{N} \right) (X_2 + X_{12}) - \beta \left(\frac{NY_1}{K} \right) - (b + v_1) Y_1 \quad (4)$$

In the 2-1-1 model the total population of ticks was represented by V with a single species of ticks notated with X . Where X_i represented the number of ticks infected with pathogen i . In order to extend this to a 2-2-1 model, instead of having a single species of ticks, two species of ticks are described by adding two additional terms: (i) W to represent the total number of the second species of ticks, and (ii) Z_i to represent the number of W ticks infected with pathogen i . Then, Equation 4 is again extended to model the introduction of the second vector population in Equation 5.

$$\begin{aligned} \frac{dY_1}{dt} = & A_1^V \left(\frac{N - Y_1 - Y_2 - Y_{12}}{N} \right) (X_1 + X_{12}) + A_1^W \left(\frac{N - Y_1 - Y_2 - Y_{12}}{N} \right) (Z_1 + Z_{12}) + v_{12 \rightarrow 1} Y_{12} \\ & - A_{12}^V \left(\frac{Y_1}{N} \right) (X_2 + X_{12}) - A_{12}^W \left(\frac{Y_1}{N} \right) (Z_2 + Z_{12}) - \beta \left(\frac{NY_1}{K} \right) - (b + v_1) Y_1 \end{aligned} \quad (5)$$

Similarly, Equation 6 models coinfection dynamics in the presence of two pathogens infecting a single tick.

$$\begin{aligned} \frac{dY_{12}}{dt} = & A_{12}^V \left(\frac{Y_1}{N} \right) (X_2 + X_{12}) + A_{12}^W \left(\frac{Y_1}{N} \right) (Z_2 + Z_{12}) + A_{21}^V \left(\frac{Y_2}{N} \right) (X_1 + X_{12}) \\ & + A_{21}^W \left(\frac{Y_2}{N} \right) (Z_1 + Z_{12}) - \beta \left(\frac{NY_{12}}{K} \right) - (b + v_{12 \rightarrow 1} + v_{12 \rightarrow 2}) Y_{12} \end{aligned} \quad (6)$$

2.3 Host-to-Tick Transmission Dynamics

This model system includes pathogen transmission mechanics that may flow in the opposing direction rather than from the infected tick to the susceptible host. In some cases, non-infected ticks which feed on infected hosts can acquire infection with either (or both) of the pathogens present in the host system, which is modeled by Equation 7. As an additional unique feature of tick biology, adult female ticks which are infected with pathogens can pass infection on to her offspring via vertical inheritance, known as transovarial transmission. Likewise, ticks which molt from one life stage to the next also carry over any infections post-molt, called transstadial transmission. Expressions for both mechanisms are included in the following model equations.

$$\begin{aligned} \frac{dX_1}{dt} = & \hat{A}_1^V \left(\frac{Y_1 + Y_{12}}{N} \right) (V - X_1 - X_2 - X_{12}) + \hat{\beta}_t^V (\gamma_1^V X_1 + \gamma_{12}^V X_{12}) + \mu_1^V \left(\frac{X_1 + X_{12}}{V} \right) (V - X_1 \\ & - X_2 - X_{12}) + \mu_1^W \left(\frac{Z_1 + Z_{12}}{W} \right) (V - X_1 - X_2 - X_{12}) - \hat{A}_{1 \rightarrow 12}^V \left(\frac{Y_2 + Y_{12}}{N} \right) X_1 \\ & - \mu_{1 \rightarrow 12}^V \frac{X_2 + X_{12}}{V} X_1 - \mu_{1 \rightarrow 12}^W \frac{Z_2 + Z_{12}}{W} X_1 - \hat{\beta} \frac{V X_1}{MN} - \hat{b} X_1 \end{aligned} \quad (7)$$

Equation 8 models coinfection dynamics in the presence of two pathogens.

$$\begin{aligned} \frac{dX_{12}}{dt} = & \hat{A}_{12} \left(\frac{Y_2 + Y_{12}}{N} \right) X_1 + \hat{A}_{21} \left(\frac{Y_1 + Y_{12}}{N} \right) X_2 + \mu_{12}^V \left(\frac{X_2 + X_{12}}{V} \right) X_1 + \mu_{21}^V \left(\frac{X_1 + X_{12}}{V} \right) X_2 \\ & + \mu_{12}^W \left(\frac{Z_2 + Z_{12}}{W} \right) X_1 + \mu_{21}^W \left(\frac{Z_1 + Z_{12}}{W} \right) X_2 - \hat{\beta}_{12}^V \frac{VX_{12}}{MN} - \hat{b}_{12}^V X_{12} \end{aligned}$$

Additional equations and code for model extensions for a 3 pathogen/1 vector/1 host (3-1-1) and 2 pathogen/1 vector/2 host (2-1-2) model system are included in the Github repository (8) associated with this study (https://github.com/hseabolt/vectorborne_SIR).

2.3 State Descriptions and Initial Values

Initial values for the base 2-1-1 model are given in Table 1 of White et al. (2019). These initial conditions have been derived from previously published models and available real-world data including field sampling of ticks by prior researchers (Gaff and Gross 2007). We have reproduced and extended Table 1 to include additional state variables applicable to the planned model extensions (below). Descriptions of initial SIR parameter values, such as transmission and recovery rates, are given in Supplemental Tables 1-3 at the end of this document for brevity. For the third pathogen in the 3-1-1 model, initial values were adapted from published prevalence and virulence data of *Rickettsia rickettsii*, the causative agent of Rocky Mountain Spotted Fever (Infante 2017). All other initial values are defined following original values given in White et al. 2019 and subject to refinement pending additional literature search. Figure 1 illustrates the compartment model states and the routes of transmission between them.

State Variable	Description	Initial Value	Model Extension
N	Total Number of Hosts	20	
N₁	Number of Host Species 1	10	2-1-2
N₂	Number of Host Species 2	10	2-1-2
V	Total Number of Ticks	4000	
V₁	Number of Vector Species 1	3000	2-2-1
V₂	Number of Vector Species 2	1000	2-2-1
Y₁	Number of Hosts Infected with Pathogen 1	1	
X₁	Number of Ticks Infected with Pathogen 1	200	
Y₂	Number of Hosts Infected with Pathogen 2	0	
X₂	Number of Ticks Infected with Pathogen 2	150	
Y₃	Number of Hosts Infected with Pathogen 3	0	3-1-1
X₃	Number of Ticks Infected with Pathogen 3	175	3-1-1
Y₁₂	Number of Coinfected Hosts with Pathogens 1,2	0	
X₁₂	Number of Coinfected Ticks with Pathogens 1,2	10	
Y₁₃	Number of Coinfected Hosts with Pathogens 1,3	0	3-1-1

X_{13}	Number of Coinfected Ticks with Pathogens 1,3	10	3-1-1
Y_{23}	Number of Coinfected Hosts with Pathogens 2,3	0	3-1-1
X_{23}	Number of Coinfected Ticks with Pathogens 2,3	5	3-1-1
Y^*	Number of Coinfected Hosts with Pathogens 1,2,3	0	3-1-1
X^*	Number of Coinfected Ticks with Pathogens 1,2,3	1	3-1-1

Table 1: Description of state variables according to proposed model extensions (partially reproduced from White et al. 2019). Rows using gray highlighting indicate new state variables unique to this study. Text is additionally colored to visually separate states unique to specific model extensions.

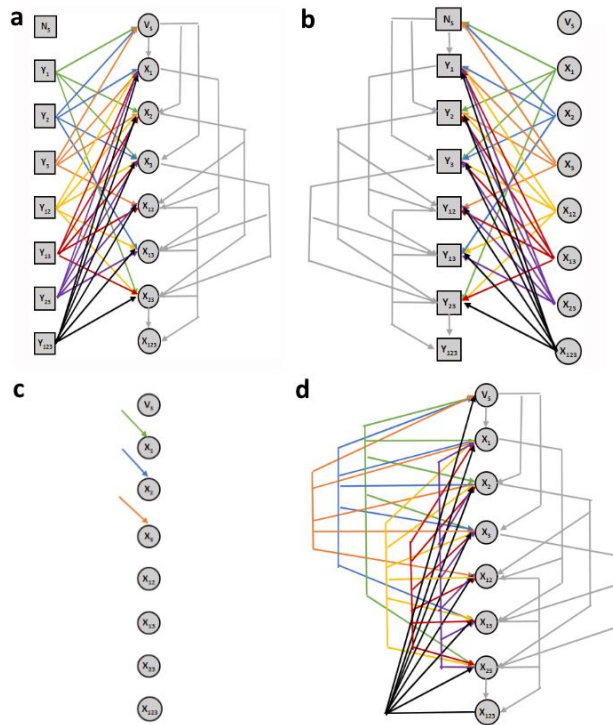


Figure 1 (left): Extended compartment model diagram showing transitions as potential routes of transmission. The colored and black lines represent the transmission of a pathogen from one organism to another. The grey lines represent the transition of an organism from one epidemiological compartment to the next. We assume that in all cases a coinfected tick will only transmit one of its pathogens at a time. Sub-figure a) Outlines Host to Tick transmission flow, b) Outlines Tick to Host transmission flow, c) Outlines Transovarial and Transstadial transmission within the model, d) Outlines how transmission can occur via tick cofeeding

2.4 Model Assumptions

In these model extensions, we have made the simplifying assumptions that all ticks have an equal ability to acquire and/or transmit infection regardless of life stage. We have made the additional assumptions that (a) infection with any pathogen is not fatal to the acquiring host and that birth/death rates among tick vectors and hosts are independent of one another, and (b) with respect to the biology and natural history of the tick vectors in our model extensions, we simplified model states for the transstadial and transovarial pathogen transmission since these introduce substantial complexity into the ODE model that were expected to ultimately encapsulate minor differences in resulting transmission patterns.

2.5 Model Dynamics

In this 2-2-1 extension, the basic reproductive numbers for vector-to- vector transmission are characterized by two equations:

$$R_{Vi} = \gamma_{Vi} + \frac{\mu_{Vi}}{\hat{\beta}_V} \quad (9)$$

$$R_{Wi} = \gamma_{Wi} + \frac{\mu_{Wi}}{\hat{\beta}_W}$$

Then, following algebraic manipulation to account for both vector populations, R_i^V and R_i^W are combined into a single R_i , calculated as a weighted average between R_i^V and R_i^W , where the weighting is determined by a number of ticks at a certain point in time (\tilde{V} , \tilde{W})

$$R_i = \frac{\tilde{V} * R_i^V + \tilde{W} * R_i^W}{\tilde{V} + \tilde{W}} \quad (10)$$

3. RESULTS AND DISCUSSION

3.1 Model simulations using three model extensions

In all three model extensions, simulations used initial values provided in White et.al (2009), Gaff and Gross (2007) publications. Figure 2 below illustrates the obtained host and vector population curves from the 2 pathogens/2 vectors/1 host (2-2-1) model simulations. One of the simplifying assumptions of this model is that infection with any pathogen is not fatal to the host, thus the total population size N remained constant throughout the simulation. By approximately 12 months, nearly all hosts had become co-infected with both pathogens, eventually displacing all uninfected hosts and hosts infected with only one pathogen. Interestingly, we observed that the population sizes of some host compartments dropped below zero in our simulations, which we believe is an artefact of the simplifying assumptions made regarding the non-fatal nature of the infected model states. Conversely, for the two vector populations, the number of both vectors infected with either of Pathogen 1 or Pathogen 2 was the same, with the curve saturating around a compartment size of 500 ticks for both vector species (X1, X2, Z1, Z2 curves, all overlap). The compartment containing ticks coinfecting with both pathogens is comparatively smaller, indicated that coinfecting hosts are rare in the vector populations.

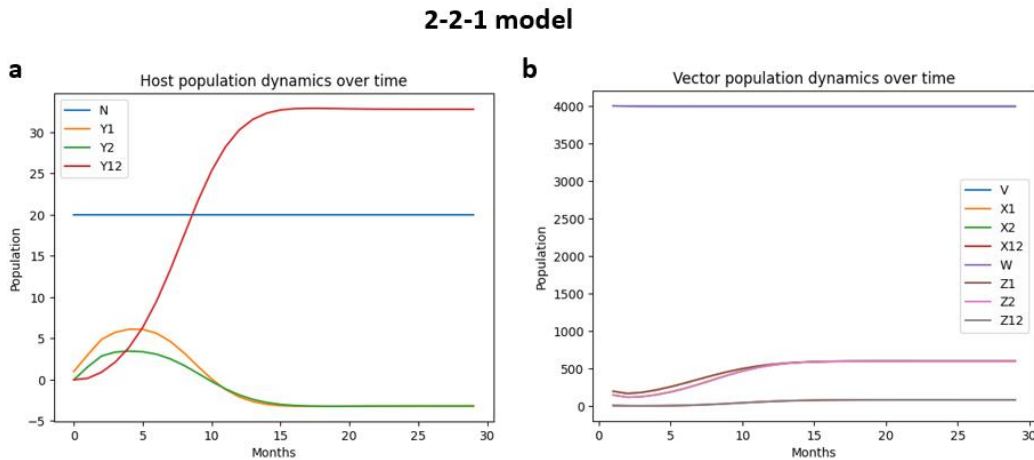


Figure 2: Host and vector population dynamics curves obtained from simulations of the 2-2-1 model extension.

Similarly the observed curves in Figure 2 for the 2-2-1 model, similar trends were observed in the 2 pathogens/1 vector/2 host (2-1-2) model, in which all hosts eventually became coinfectd with both pathogens despite the infected vector population remaining comparatively rare. 2-1-2 model simulation curves are shown in Figure 3.

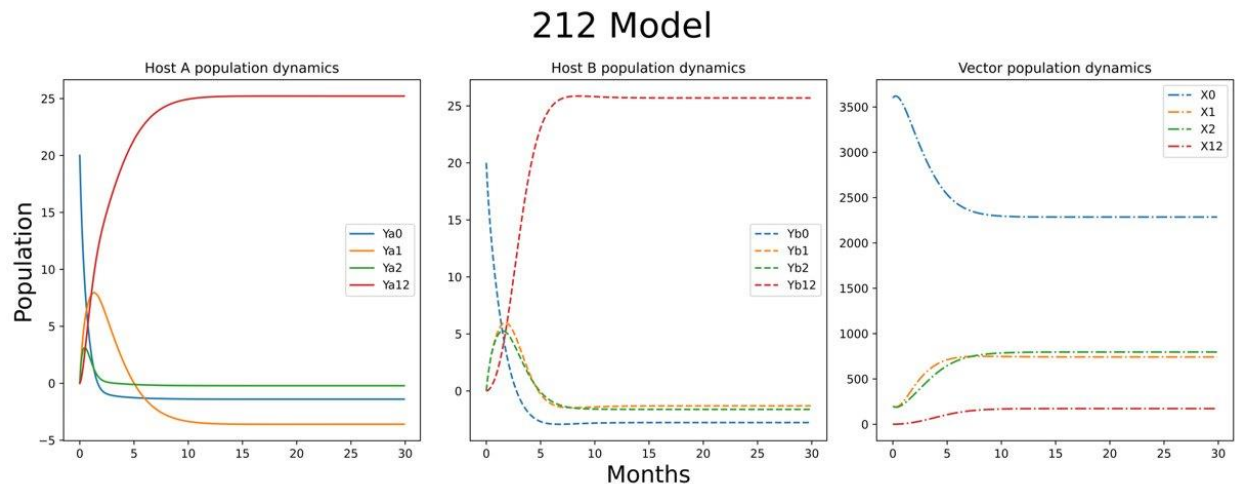


Figure 3: Host and vector population dynamics curves obtained from simulations of the 2-1-2 model extension.

The model extension that introduced a third pathogen to the system (3-1-1 model), revealed much more varied population dynamics among the vector population. In this scenario, while there is only one tick vector, the population dynamics are the most complex. The susceptible compartment decreased at a slowing rate over the course of the simulation, while all combinations of one or two pathogens displayed trends in which the number of ticks infected with any of these pathogen combinations reached a peak and then decreased, as the total number of vectors coinfectd with all three pathogens continued to steadily rise. Like the other model extensions that revealed that vectors coinfectd with multiple pathogens were comparatively rare in the total vector population(s), the same trend was observed in this simulation, with the interesting exception of coinfection of all three pathogens, which eventually overtook all other possible infected compartments to be the most prevalent infected state. At no point, however, does this 3-pathogen coinfectd state surpass the susceptible tick population, and both curves show decaying rates of change at the end of the simulation time steps. It remains undetermined if the 3-pathogen coinfectd state would eventually surpass the susceptible population or saturate out to a stable plateau.

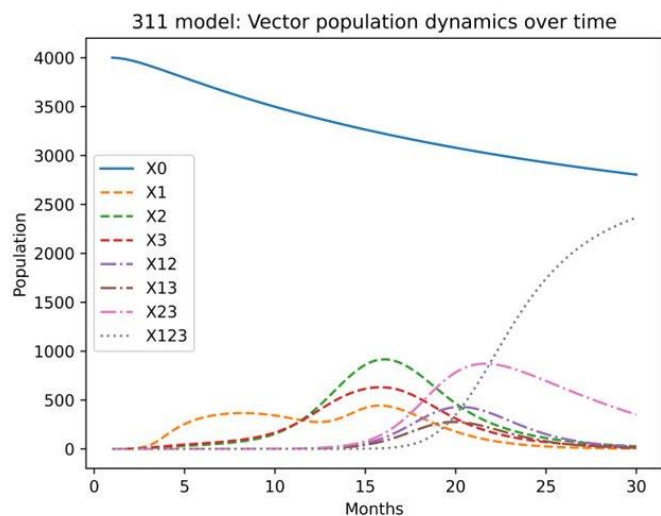


Figure 4: Host and vector population dynamics curves obtained from simulations of the 3-1-1 model extension.

3.2 Study Limitations

A key limitation of this study is the dearth of available real-world data regarding the prevalence of *Rickettsia* pathogens in diverse tick populations. We were only able to obtain a limited amount of data from which to attempt model calibrations, which ultimately proved unsuccessful due to conflicting initial value parameters needed for successful model simulations. In addition to the limiting factors necessitating us to rely on a small number of model studies to derive parameters for our model extensions, some of the simplifying assumptions made during the course of deriving equations for the model extensions proved to have implications for the model, such as some host compartments returning negative values, which is biologically impossible.

4. CONCLUSIONS

The goals of this study were to simulate and examine the effects on transmission dynamics between competing *Rickettsia* pathogens by extending the 2-1-1 SIR compartment model outlined in White et al. (2019) to three additional compartment models that introduced new biologic diversity in the form of a new pathogen (3-1-1 model), a new vector species capable of transmitting pathogens (2-2-1 model), and lastly, a new host that acts as a reservoir species for vector-borne pathogens (2-1-2 model). In all three of our model simulations, our results revealed that host coinfection with multiple pathogens became the most prevalent outcome despite co-infected ticks themselves being comparatively quite rare in the vector populations. We can surmise from the model curves in Figures 2-4 that indeed, in all cases, the pathogens persist over time, eventually coinfecting the same host. We were unsuccessful in directly comparing the basic reproductive and invasion reproductive numbers for each of these models as a second line of evidence via analysis.

Future work on this study should include completion of the analysis to compare reproductive numbers between these model extensions, as well as to published vector-borne SIR models like the 2-1-1 model described in White et al (2009). These models should be additionally calibrated using (a) real-world data to the extent possible and/or (b) in the absence of suitable real-world data, calibrated using a range of plausible values to determine a range of expected values for the model curves under different conditions. Further, additional analysis of these model extensions should be undertaken, for example, using phase plane analysis to determine potential equilibria points and stability.

5. DATA AVAILABILITY AND ACKNOWLEDGEMENTS

All project materials, documentation, and code can be retrieved from Github (https://github.com/hseabolt/vectorborne_SIR). We are grateful to the reviewer(s) for providing excellent feedback on the initial proposal and milestone report that helped to improve this research further.

6. REFERENCES

1. White A, Schaefer E, Thompson CW, Kribs CM, Gaff H (2019). Dynamics of two pathogens in a single tick population. *Lett Biomath*, 6(1):50-66.

2. Gaff HD, & Gross LJ (2007). Modeling tick-borne disease: a metapopulation model. *Bulletin of Mathematical Biology*, 69(1), 265–288.
3. Infante GPP (2017). Modelling and stochastic simulation to study the dynamics of *Rickettsia rickettsia* in populations of *Hydrochaerus hydrochaerus* and *Amblyomma sculptum* in the State of Sao Paulo, Brazil [Unpublished PhD thesis]. University of Sao Paulo.
4. URL: <https://www.cdc.gov/ticks/>
5. Durden LA, & Beati L (2013). Modern tick systematics. *Biology of Ticks*, 1, 17-58.
6. Rodino KG, Theel ES, & Pritt BS (2020). Tick-borne diseases in the United States. *Clinical Chemistry*, 66(4), 537-548.
7. Madison-Antenucci S, Kramer LD, Gebhardt LL, & Kauffman E (2020). Emerging tick-borne diseases. *Clinical microbiology reviews*, 33(2), e00083-18.

APPENDIX B: SUPPLEMENTARY TABLES

Parameter	Description	Initial Value	Model Extension
$\hat{A}1$	Host-to-Tick Pathogen 1 Transmission Rate	0.07	
$\hat{A}2$	Host-to-Tick Pathogen 2 Transmission Rate	0.07	
$\hat{A}3$	Host-to-Tick Pathogen 3 Transmission Rate	0.07	3-1-1
$\hat{A}12$	Host-to-Tick Coinfection Transmission Rate Pathogens 1,2	0.035	
$\hat{A}13$	Host-to-Tick Coinfection Transmission Rate Pathogens 1,3	0.035	3-1-1
$\hat{A}23$	Host-to-Tick Coinfection Transmission Rate Pathogens 2,3	0.035	3-1-1
A1	Tick-to-Host Pathogen 1 Transmission Rate	0.02	
A2	Tick-to-Host Pathogen 2 Transmission Rate	0.02	
A3	Tick-to-Host Pathogen 3 Transmission Rate	0.02	3-1-1
A12	Tick-to-Host Coinfection Transmission Rate Pathogens 1,2	0.01	
A13	Tick-to-Host Coinfection Transmission Rate Pathogens 1,3	0.01	3-1-1
A23	Tick-to-Host Coinfection Transmission Rate Pathogens 2,3	0.01	3-1-1
$\gamma1$	Tick Transovarial and Transstadial Transmission of Pathogen 1	0.4	
$\gamma2$	Tick Transovarial and Transstadial Transmission of Pathogen 2	0.4	
$\gamma3$	Tick Transovarial and Transstadial Transmission of Pathogen 3	0.4	3-1-1
$\gamma12$	Coinfected Tick Transovarial and Transstadial Transmission (1,2)→1	0.2	
$\gamma21$	Coinfected Tick Transovarial and Transstadial Transmission (1,2)→2	0.2	3-1-1
$\gamma13$	Coinfected Tick Transovarial and Transstadial Transmission (1,3)→1	0.2	3-1-1
$\gamma31$	Coinfected Tick Transovarial and Transstadial Transmission (1,3)→3	0.2	3-1-1
$\gamma23$	Coinfected Tick Transovarial and Transstadial Transmission (2,3)→2	0.2	3-1-1
$\gamma32$	Coinfected Tick Transovarial and Transstadial Transmission (2,3)→3	0.2	3-1-1

μ_1	Tick Cofeeding Transmission Rate of Pathogen 1	0.01	
μ_2	Tick Cofeeding Transmission Rate of Pathogen 2	0.01	
μ_2	Tick Cofeeding Transmission Rate of Pathogen 3	0.01	3-1-1
μ_{12}	Tick Cofeeding Coinfection Transmission Rate Pathogens 1,2	0.005	
μ_{13}	Tick Cofeeding Coinfection Transmission Rate Pathogens 1,3	0.005	3-1-1
μ_{23}	Tick Cofeeding Coinfection Transmission Rate Pathogens 2,3	0.005	3-1-1
ν_1	Host Recovery Rate for Pathogen 1	0.166	
ν_2	Host Recovery Rate for Pathogen 2	0.166	
ν_3	Host Recovery Rate for Pathogen 3	0.166	3-1-1
ν_{12}	Host Recovery Rate of Coinfection Pathogens (1,2)→1	0.166	
ν_{21}	Host Recovery Rate of Coinfection Pathogens (1,2)→2	0.166	
ν_{23}	Host Recovery Rate of Coinfection Pathogens (2,3)→2	0.166	3-1-1
ν_{32}	Host Recovery Rate of Coinfection Pathogens (2,3)→3	0.166	3-1-1
ν_{13}	Host Recovery Rate of Coinfection Pathogens (1,3)→1	0.166	3-1-1
ν_{31}	Host Recovery Rate of Coinfection Pathogens (1,3)→3	0.166	3-1-1
K	Host Carrying Capacity	20	
M	Maximum Ticks per Host	200	
β	Host Population Growth Rate	0.2	
β	Tick Population Growth Rate	0.75	
b	Host Background Density-Independent Mortality Rate	0	
\hat{b}	Tick Background Density-Independent Mortality Rate	0.001	

Table S1: SIR model parameters and initial values for the base 2-1-1 and extended 3-1-1 model (partially reproduced from White et al. 2019). Rows using gray highlighting indicate new state variables unique to this study. Wherever possible, variable symbols follow White et al. (2019).

Parameter	Description	Initial Value	Model Extension
\hat{A}_{11}	Host1-to-Tick Pathogen 1 Transmission Rate	0.07	
\hat{A}_{21}	Host2-to-Tick Pathogen 1 Transmission Rate	0.07	2-1-2
\hat{A}_{12}	Host1-to-Tick Pathogen 2 Transmission Rate	0.07	
\hat{A}_{22}	Host2-to-Tick Pathogen 2 Transmission Rate	0.07	2-1-2
\hat{A}^*1	Host1-to-Tick Coinfection Transmission Rate Pathogens 1,2	0.035	
\hat{A}^*2	Host2-to-Tick Coinfection Transmission Rate Pathogens 1,2	0.035	2-1-2
A11	Tick-to-Host1 Pathogen 1 Transmission Rate	0.02	
A21	Tick-to-Host2 Pathogen 1 Transmission Rate	0.02	2-1-2
A12	Tick-to-Host1 Pathogen 2 Transmission Rate	0.02	
A22	Tick-to-Host2 Pathogen 2 Transmission Rate	0.02	2-1-2
A*1	Tick-to-Host1 Coinfection Transmission Rate Pathogens 1,2	0.01	
A*2	Tick-to-Host2 Coinfection Transmission Rate Pathogens 1,2	0.01	2-1-2
γ_1	Tick Transovarial and Transstadial Transmission of Pathogen 1	0.4	
γ_2	Tick Transovarial and Transstadial Transmission of Pathogen 2	0.4	
γ_{12}	Coinfected Tick Transovarial and Transstadial Transmission (1,2)→1	0.2	
μ_1	Tick Cofeeding Transmission Rate of Pathogen 1	0.01	
μ_2	Tick Cofeeding Transmission Rate of Pathogen 2	0.01	
μ_{12}	Tick Cofeeding Coinfection Transmission Rate Pathogens 1,2	0.005	
v11	Host1 Recovery Rate for Pathogen 1	0.166	
v12	Host1 Recovery Rate for Pathogen 2	0.166	2-1-2
v21	Host2 Recovery Rate for Pathogen 2	0.166	
v22	Host2 Recovery Rate for Pathogen 2	0.166	2-1-2
v11	Host1 Recovery Rate of Coinfection Pathogens (1,2)→1	0.166	
v12	Host1 Recovery Rate of Coinfection Pathogens (1,2)→2	0.166	
v21	Host2 Recovery Rate of Coinfection Pathogens (1,2)→1	0.166	2-1-2
v22	Host2 Recovery Rate of Coinfection Pathogens (1,2)→2	0.166	2-1-2
K1	Host1 Carrying Capacity	20	
K2	Host2 Carrying Capacity	20	2-1-2
M	Maximum Ticks per Host	200	
β_1	Host1 Population Growth Rate	0.2	
β_2	Host1 Population Growth Rate	0.2	2-1-2
β	Tick Population Growth Rate	0.75	
b1	Host1 Background Density-Independent Mortality Rate	0.01	
b2	Host2 Background Density-Independent Mortality Rate	0.01	2-1-2
\hat{b}	Tick Background Density-Independent Mortality Rate	0.001	

Table S2: SIR model parameters and initial values for the base 2-1-1 and extended 2-1-2 (2 pathogen, 1 vector, 2 hosts) model, partially reproduced from White et al. 2019. Rows using gray highlighting indicate new state variables unique to this study. Wherever possible, variable symbols follow White et al. (2019).

Parameter	Description	Initial Value	Model Extension
\hat{A}_{11}	Host-to-Tick1 Pathogen 1 Transmission Rate	0.07	
\hat{A}_{12}	Host-to-Tick1 Pathogen 2 Transmission Rate	0.07	
\hat{A}_{21}	Host-to-Tick2 Pathogen 1 Transmission Rate	0.07	2-2-1
\hat{A}_{22}	Host-to-Tick2 Pathogen 2 Transmission Rate	0.07	2-2-1
\hat{A}^*1	Host-to-Tick1 Coinfection Transmission Rate Pathogens 1,2	0.035	
\hat{A}^*2	Host-to-Tick2 Coinfection Transmission Rate Pathogens 1,2	0.035	2-2-1
A11	Tick1-to-Host Pathogen 1 Transmission Rate	0.02	
A12	Tick1-to-Host Pathogen 2 Transmission Rate	0.02	
A21	Tick2-to-Host Pathogen 1 Transmission Rate	0.02	2-2-1
A22	Tick2-to-Host Pathogen 2 Transmission Rate	0.02	2-2-1
A*1	Tick1-to-Host Coinfection Transmission Rate Pathogens 1,2	0.01	
A*2	Tick2-to-Host Coinfection Transmission Rate Pathogens 1,2	0.01	2-2-1
γ_{11}	Tick1 Transovarial and Transstadial Transmission of Pathogen 1	0.4	
γ_{12}	Tick1 Transovarial and Transstadial Transmission of Pathogen 2	0.4	
γ^*1	Coinfected Tick1 Transovarial and Transstadial Transmission (1,2)→1	0.2	
γ_{21}	Tick2 Transovarial and Transstadial Transmission of Pathogen 1	0.6	2-2-1
γ_{22}	Tick2 Transovarial and Transstadial Transmission of Pathogen 2	0.6	2-2-1
γ^*2	Coinfected Tick2 Transovarial and Transstadial Transmission (1,2)→1	0.3	2-2-1
μ_{11}	Tick1 Cofeeding Transmission Rate of Pathogen 1	0.01	
μ_{12}	Tick1 Cofeeding Transmission Rate of Pathogen 2	0.01	
μ^*1	Tick1 Cofeeding Coinfection Transmission Rate Pathogens 1,2	0.005	
μ_{21}	Tick2 Cofeeding Transmission Rate of Pathogen 1	0.02	2-2-1
μ_{22}	Tick2 Cofeeding Transmission Rate of Pathogen 2	0.02	2-2-1
μ^*2	Tick2 Cofeeding Coinfection Transmission Rate Pathogens 1,2	0.1	2-2-1
v1	Host Recovery Rate for Pathogen 1	0.166	
v2	Host Recovery Rate for Pathogen 2	0.166	
v12	Host Recovery Rate of Coinfection Pathogens (1,2)→1	0.166	
v21	Host Recovery Rate of Coinfection Pathogens (1,2)→2	0.166	
K	Host Carrying Capacity	20	
M1	Maximum Ticks1 per Host	150	
M2	Maximum Ticks2 per Host	50	2-2-1
β	Host Population Growth Rate	0.2	
β_1	Tick1 Population Growth Rate	0.75	
β_2	Tick2 Population Growth Rate	0.75	2-2-1
b	Host Background Density-Independent Mortality Rate	0	
\hat{b}_1	Tick1 Background Density-Independent Mortality Rate	0.001	
\hat{b}_2	Tick2 Background Density-Independent Mortality Rate	0.001	2-2-1

Table S3: SIR model parameters and initial values for the base 2-1-1 and extended 2-2-1 (2 vector) model, partially reproduced from White et al. 2019. Rows using gray highlighting indicate new state variables unique to this study. Wherever possible, variable symbols follow White et al. (2019).